CHAPTER 6 - FINITE ELEMENT MODELLING OF CENOZOIC STRESS FIELDS IN THE IBERIAN PENINSULA

Based on the reconstructions presented in Chapter 4 and 5, geometry and boundary conditions can be obtained to construct numerical models of the (paleo)stress fields for different stages in the evolution of the Iberian Peninsula. Periods for which numerical models were constructed have been selected based on the following criteria:

1. completeness of the reconstructed stress field:

To enable validation of the models, comparison of the results obtained by numerical modelling with the reconstructed stress field should be possible. For several periods it turned out to be impossible to construct stress fields for large parts of the studied region, either due to lack of sufficient good data or tectonic quiescence (e.g. 18 Ma). Numerical modelling has only been carried out for those periods for which a rather well constrained stress field could be reconstructed.

2. availability of first order paleotopography estimates:

A first order estimate of paleotopography is required, because topography is used to calculate crustal thickness (Chapter 2). As for the present, the paleo topography is filtered with a low-pass filter with a boundary wavelength of 100km to simulate regional isostasy and to remove local effects. Panel A in Figure 6.1 demonstrates the effect of filtering the present-day topography and shows the low level of required accuracy for paleotopography, the estimates have error bars of over 500m. This is rather convenient: estimating paleotopography is a difficult process. Paleotopography can be generated to this accuracy for only a few of the time slices of Chapter 4 and 5 (see Figure 6.1.1 panels B-E).

3. representation of the major tectonic intervals in the Iberian Peninsula:

The major tectonic intervals in the western Mediterranean have been outlined in detail in Chapter 4 and 5 and can be related to a) the Pyrenean collision, b) opening of the western part of the Mediterranean Basin, and c) collision in the Betics.

Based on these three requirements, 5 time intervals were found to be suitable for numerical modelling: 54Ma, 36Ma, 24Ma, 12Ma and present. After a short general description of the general modelling procedure, the model setup, boundary conditions and results of the mentioned time steps will be discussed.

6.1 General model description

Finite element calculations were performed using the ANSYS© software package. The models consist of triangular (type: SOLID92) elastic shell elements. Element thickness is 100km and typical element edge length in the area of interest is 100km. The models were constructed in a spherical coordinate system with longitude, latitude and Earth's radius as xyz-coordinates. This is done to avoid errors in the geometry and direction of forces related to ridge push in the higher latitude regions. A frame was added around the free boundaries of the model to minimize edge effects, following Bada [1999]. Poisson's ratio (v) is kept constant at 0.25 for all of the models. To simulate differences in material properties, Young's Modulus has been varied for the different crustal types as defined in the models for the calculation of stresses induced by density differences. Basically, two material settings were applied: (a) a constant Young's modulus throughout the entire model or (b) different Young's modulus for five areas: (1) young oceanic crust, (2) old oceanic crust, (3) thinned continental, (4) elevated continental and (5) surrounding

frame. The elements in the mesh are assigned to be of any of the five types, depending on their location. The limit between oceanic and thinned continental coincides with the boundary between both as adopted by Stapel [1999]. Several routines were developed to calculate the magnitude of forces that have to be applied to the nodes of the models based on two parameters: the general value of the force per unit length for the specified boundary segment and the orientation of the force at every single node.
The model results using the assumed geometries and activity at plate boundaries as derived from paleogeographical studies will be compared with the reconstructed stress fields for the different time slices. This comparison provides a quantitative test of the numerous qualitative paleogeographical concepts proposed for the tectonic evolution of the Iberian Peninsula and surrounding western Mediterranean. The models for 12Ma, 24Ma and 36Ma will show the important consequences on the stress field when choosing different tectonic scenarios.

At first, an attempt was made to obtain a first order fit using the geometries resulting from the reconstructions in Chapter 4, always starting with the inferred boundary conditions.
In the first runs, ridge push forces were calculated using the formulas described in Appendix A. To the best fitting scenario, stresses induced by lateral density variations are added. Their effect is discussed in the light of the changes they produce with respect to the first set of results.

6.2 Present-day stress field

The best constraints on any of the (paleo)stress fields in the Iberian Peninsula are available for the present. Therefore, it is the starting point of the modelling procedure used to calibrate the applied techniques and concepts.
The general trends in the trajectories of Sh_{max} and regional state of stress within the Iberian Peninsula (see Figure 6.2.1b) have been determined by SIGMA [1998], based on a combination of focal mechanism solutions, fault-slip data and borehole breakout data. Generally, Sh_{max} is oriented ~N140 in the southern to central peninsula, with rotations to more EW-directions along the western margin and more N-S in the northeastern corner of the peninsula.
The orientation of the principal stresses and the principal stress difference ratio along the southwestern boundary of the Eurasian plate with the North American and African plates has been determined by De Vicente *et al.* [2000] by inverting focal mechanisms of earthquakes (see Figure 6.2.1a). The extension along the Mid Ocean Ridge (30º to 65º N) ranges from E-W to ESE-WSW, showing a triaxial extension. The state of stress changes to strike-slip regime in the transform fault zones, and the strike of Sh_{max} rotates clockwise to NW in the dextral strike-slip faults and counterclockwise to the NE in the sinistral ones. Along the margin between the Eurasian and African plates (from the Azores triple junction to Algeria), Sh_{max} keeps a constant NW-SE strike but the stress ratio values range from triaxial extensionin the west, to uniaxial compression in the east, passing through a strike-slip regime in the middle zone. With a NW-SE oriented Sh_{max}, strike-slip and extensional stresses prevail in most of the Iberian Peninsula, whereas southwards it is dominated by uniaxial compressive stresses.

Observations, model geometry and boundary conditions

The distribution of seismicity in the Iberian region from 1980 to present-day (as shown in Figure 2.4.1.4) has been used to determine the location of the active plate boundaries of

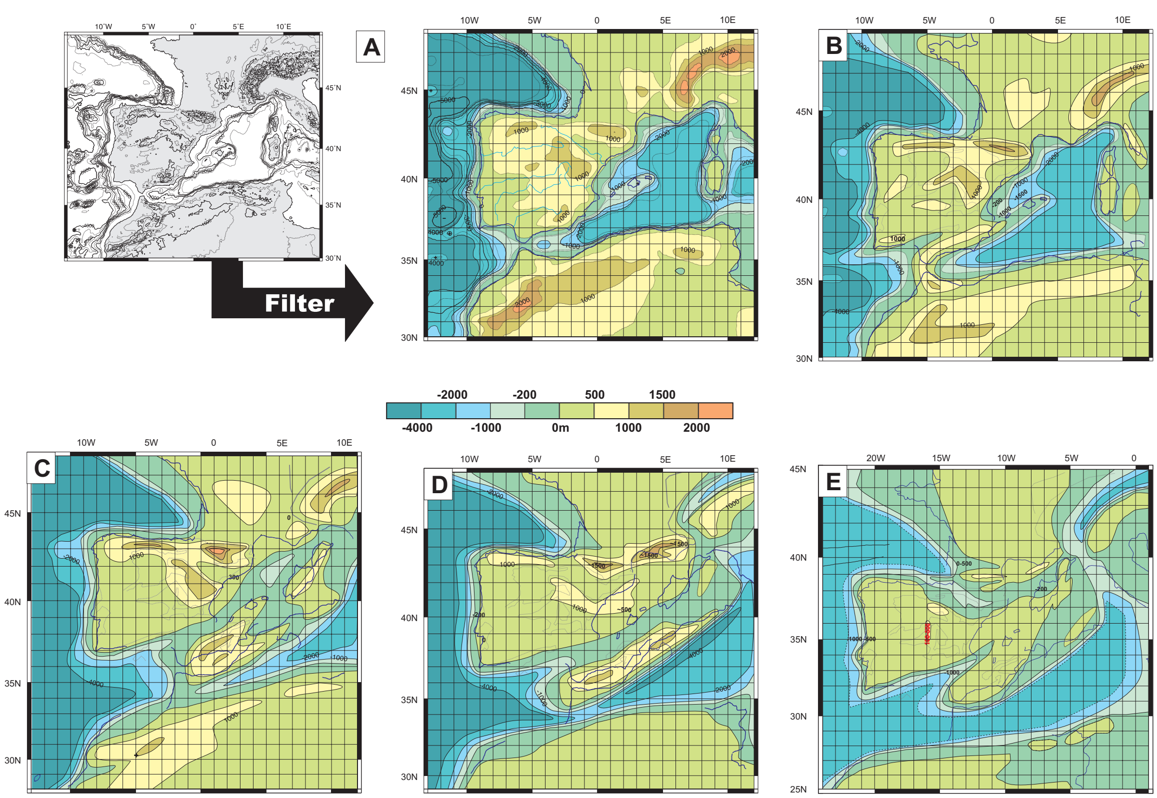

Figure 6.1.1 (see www.geo.vu.nl/~andb/iberia for full color, large size)
(Paleo) topography based on the reconstructions in Chapters 4 and 5 (accuracy at maximum 500m) filtered with a low pass filter applying a boundary wavelength of 100km to simulate regional isostasy. For the present-day situation (panel a), both the real topography (gray) and the filtered data set (color) are shown to indicate the accuracy level of the paleotopography. b) Filtered paleotopography for 12Ma, c) Filtered paleotopography for 24Ma, d) Filtered paleotopography for 36Ma and e) Filtered paleotopography for 54Ma.

Iberia. The western boundary is formed by the Mid Atlantic ridge from the Azores until north of Spitsbergen, aligned with shallow seismic activity. Ridge push forces have been calculated using the formulas described in Appendix A and are equivalent to $3.0x10^{12}$N/m along the southern part diminishing northwards to $1.5x10^{12}$N/m near Iceland and $0.8x10^{12}$N/m near Spitsbergen. The southern boundary of the model is located along the spreading Azores and Terceira ridge, which show up by superficial (<10km) seismic activity, restricted to the thin oceanic crust to the nearly aseismic Gloria Fault. From here, the exact location of the plate boundary between Africa and Eurasia/Iberia is a matter of debate. A diffuse character of the southern boundary is reflected by the alignment of deeper seated earthquakes (30-150 km, standard error for depth less than 15 km) in lower crustal levels in northern Africa to events along the Gloria Fault.

Figure 6.2.1 (Next page, after De Vicente et al. [2000]).
The orientation of the principal stresses and the principal stress difference ratio in the southwestern part of the Eurasian plate (panel a) and Iberia (panel b) determined by inversion method of focal mechanisms of earthquakes.
a) The ridge push (30º to 65º N) ranges from E-W to ESE-WSW, with R-values that show a triaxial extensional stress. The state of stress changes to strike-slip in transform fault zones, Sh_{max} turns clockwise to NW in dextral strike-slip faults and counterclockwise to NE in sinistral ones. Along the margin between the Eurasian-African plates, from the Azores triple junction to Algeria, Sh_{max} keeps a constant NW-SE strike but stress ratio values range from triaxial extensional stress state in the west, to uniaxial compressive stress state in the east, passing through an intermediate regime in between.
b) With a predominantly NW-SE oriented Sh_{max}, strike-slip and extensional stresses prevail in most of the Iberian Peninsula, whereas in the south uniaxial compressive stresses dominate.

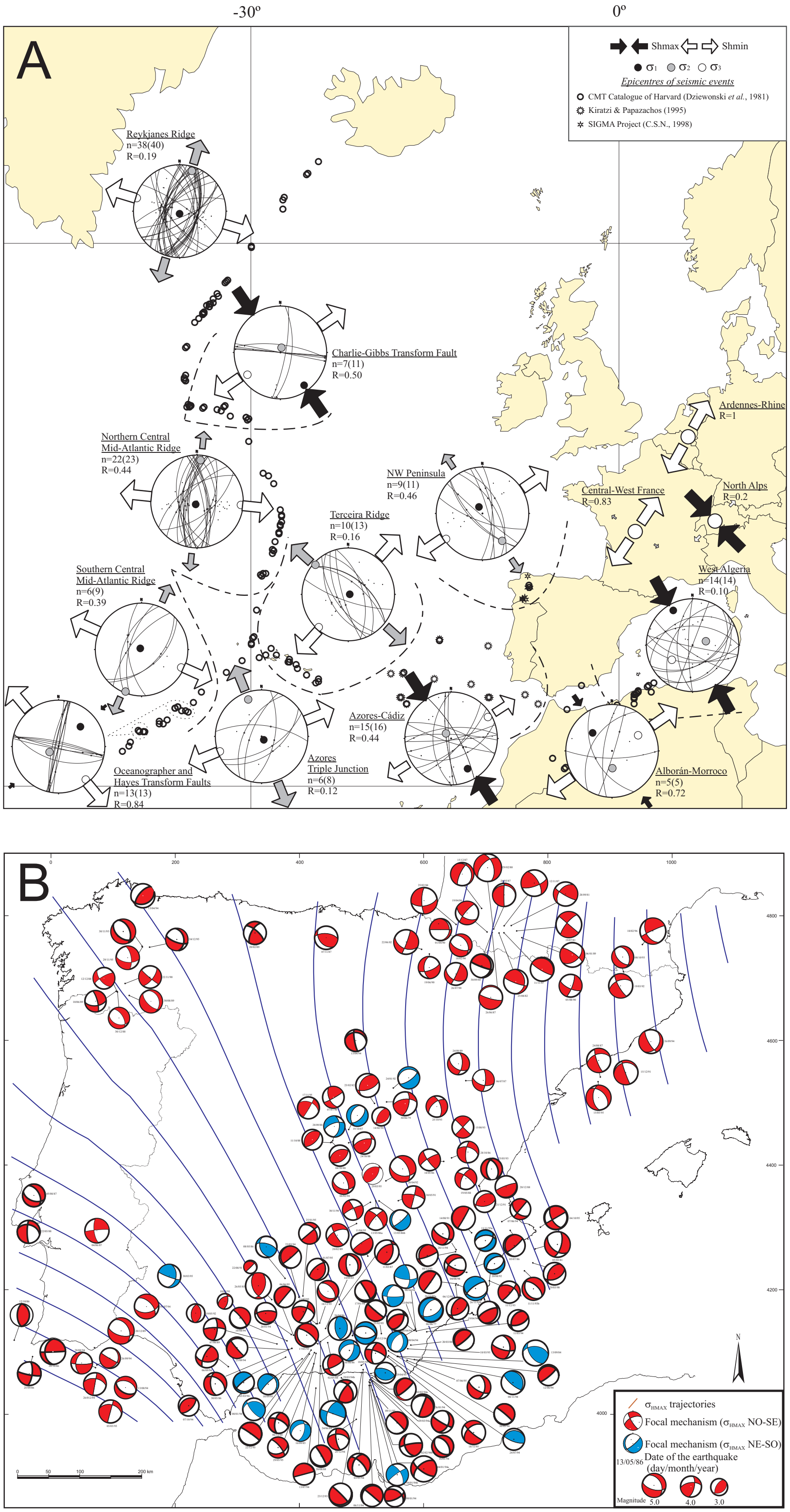
-30º
0º
60º
50º
40º
30º
A
Shmax
Shmin
σ1 σ2 σ3
Epicentres of seismic events
CMT Catalogue of Harvard (Dziewonski et al., 1981)
Kiratzi & Papazachos (1995)
SIGMA Project (C.S.N., 1998)
Reykjanes Ridge
n=38(40)
R=0.19
Charlie-Gibbs Transform Fault
n=7(11)
R=0.50
Ardennes-Rhine
R=1
Northern Central
Mid-Atlantic Ridge
n=22(23)
R=0.44
NW Peninsula
n=9(11)
R=0.46
Central-West France
R=0.83
North Alps
R=0.2
Terceira Ridge
n=10(13)
R=0.16
Southern Central
Mid-Atlantic Ridge
n=6(9)
R=0.39
West Algeria
n=14(14)
R=0.10
Azores-Cádiz
n=15(16)
R=0.44
Oceanographer and
Hayes Transform Faults
n=13(13)
R=0.84
Azores
Triple Junction
n=6(8)
R=0.12
Alborán-Morroco
n=5(5)
R=0.72
B
0
200
400
600
800
1000
4800
4600
4400
4200
4000
N
0 50 100 200 km
σHMAX trajectories
Focal mechanism (σHMAX NO-SE)
Focal mechanism (σHMAX NE-SO)
13/05/86
Date of the earthquake
(day/month/year)
Magnitude
5.0
4.0
3.0

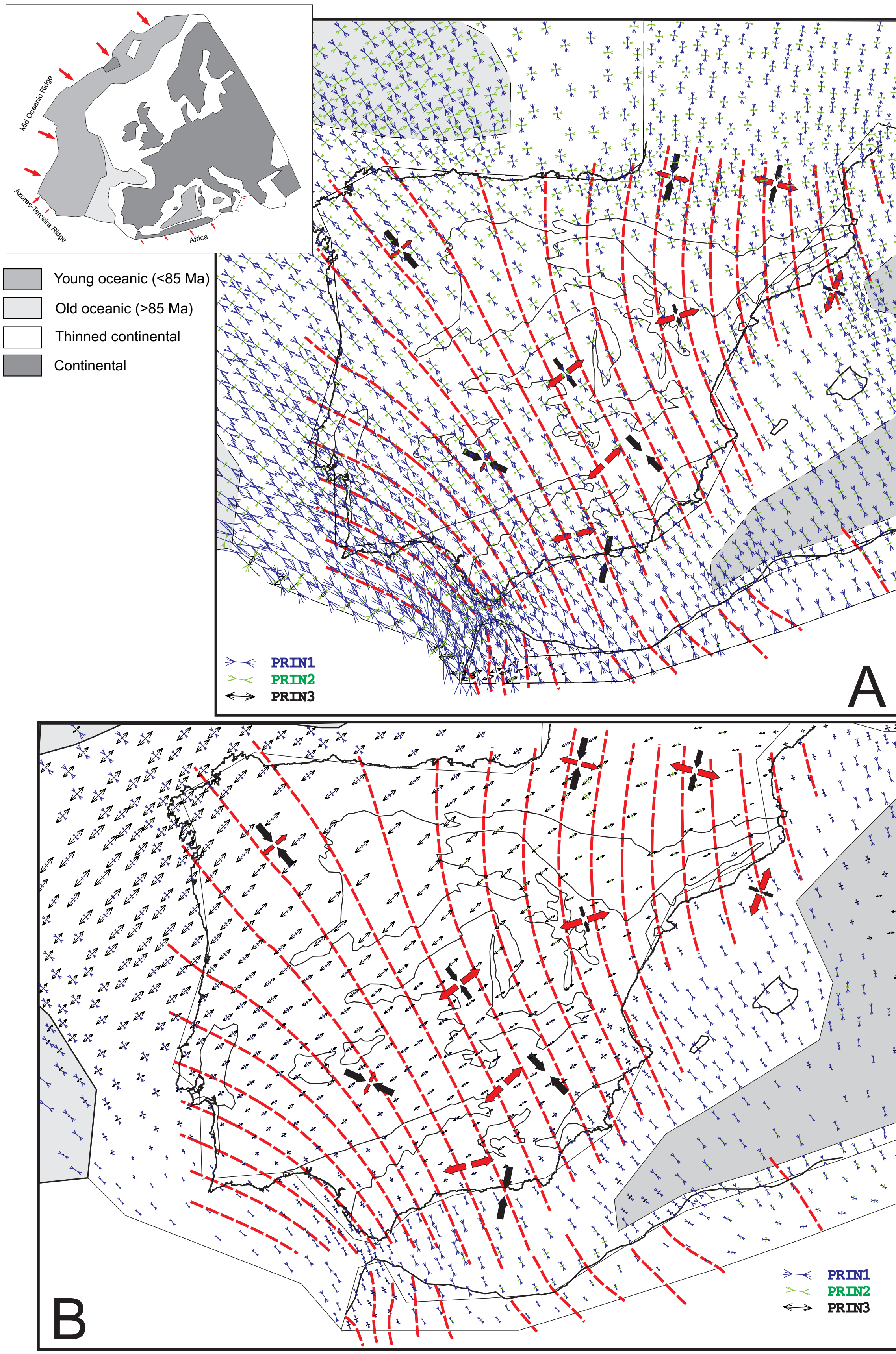
Mid Oceanic Ridge
Azores-Terceira Ridge
Africa
Young oceanic (<85 Ma)
Old oceanic (>85 Ma)
Thinned continental
Continental
PRIN1
PRIN2
PRIN3
A
PRIN1
PRIN2
PRIN3
B

Figure 6.2.2 (previous page , see www.geo.vu.nl/~andb/iberia for full size, full color version)
Figure comparing modelling results for the present-day stress field and observations of the present-day stress field. Inset shows boundary conditions and distribution of young oceanic (intermediate gray), old oceanic (light gray), continental margin (white) and elevated continental (dark gray) regions. Thick arrows and dashed lines show observed stress data and stress trajectories, small arrows show model results.
a) The only forces applied are at the boundaries of the model. Whereas the general orientation of Sh_{max} is close to the observed stress field, the local state of stress is significantly different.
b) Like (a), but with topographically induced stresses also included. Note the nearly similar orientation of Sh_{max} but better fit for the local state of stress with respect to panel a).

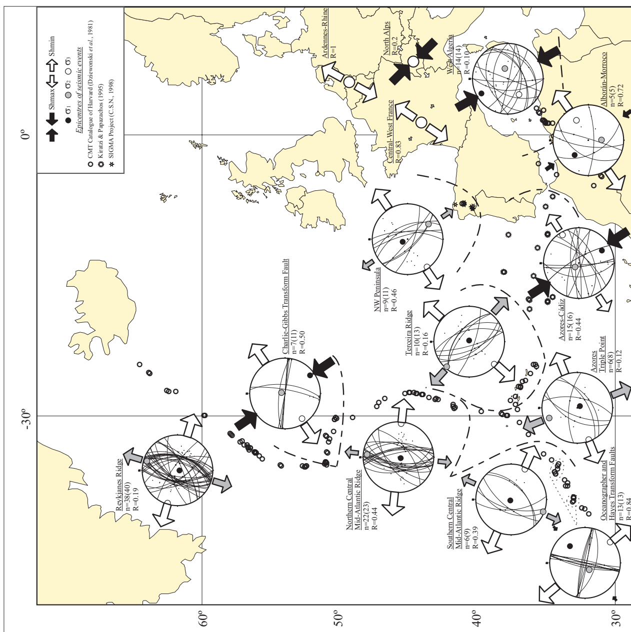

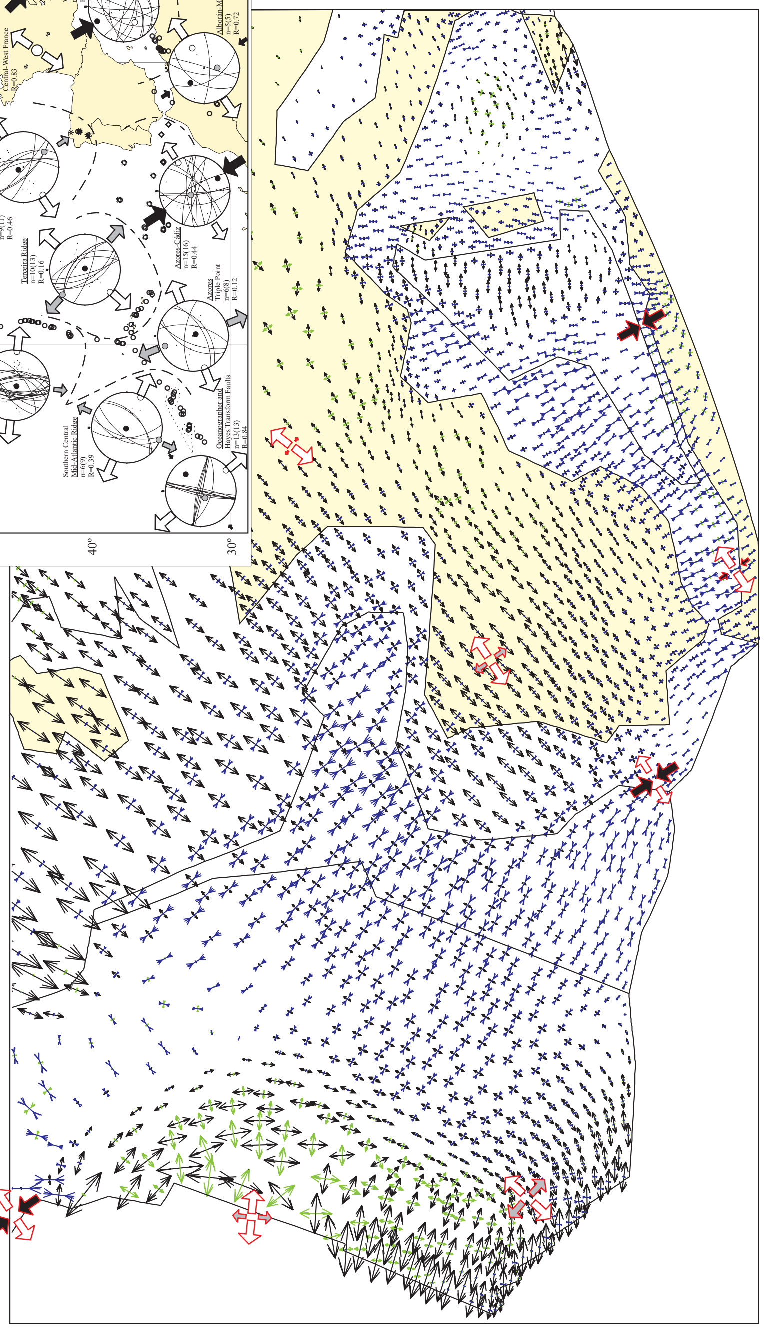

Figure 6.2.3
Results for a larger part of the model incorporating induced stresses. When the results are compared with observations on the stress field and orientation, the results fit the data in great detail (see www.geo.vu.nl/~andb/iberia for full size, full color version).

An estimate of the collision forces related to the collision of Africa and –at least the- Iberian part of Eurasia could be obtained. In the southwestern extreme of the Eurasian plate, the main boundary processes are limited to oceanic spreading and collision with Africa [Gölke & Coblentz, 1996]; [Grünthal & Stromeyer, 1992]. The magnitude and direction of the ridge push force can be determined using the formulas described in Appendix A. The direction of convergence between Africa has been estimated from magnetic anomaly patterns and seismotectonic deformation along the plate boundary [Argus *et al.*, 1989]; [Jimenéz Munt, 1999]. The direction of maximum horizontal compression is well documented in the Iberian Peninsula [SIGMA, 1998]. All this results in the fact that the only unknown in this setting is the magnitude of the collision forces related to the African-Eurasian convergence. Collision forces related to the rotational convergence of Africa-Eurasia (0.104°/Ma around a pole located at around –20°W/20°N [Argus *et al.*, 1989]) have been simulated by a decreasing force applied oriented N340° near Tunisia to oriented N270° along Gloria Fault to extension along the Terceira and Azores ridges. A few tests have been done to determine the values that predict the best fit.
The eastern boundary has been chosen along the 35°E meridian (following Gölke & Coblentz [1996]) to represent a stable border. Although this is not a plate boundary, these authors showed that its influence is acceptable for western Europe, let alone that its application would influence the pattern of stress for the southwestern part of the plate.

Model results

With respect to the orientation of Sh_{max}, the model results (see Figure 6.2.2a) closely resemble the observations (also for northern Africa and southern France), except for a misfit in the northeastern peninsula. The model does not reproduce the clockwise rotation observed in the stress field to an orientation perpendicular to the Pyrenees. An explanation for this can be the fact that the former plate boundary through the Pyrenees still constitutes a large-scale weakness zone (clearly reflected in pronounced but superficial seismic activity, see Figure 2.4.1.4). Including such a zone in the model would result in forces trending perpendicular to it, rotating the stress trajectories NNE, as is observed in the region. When taking a closer look at the results, the homogeneity of the modelled stress field is striking, which is in contrast with the observed stress regimes (larger arrows in Figure) that differ significantly from region to region.

The dominant sources of stress in this southwestern most part of the Eurasian plate are ridge push forces and collisional forces, which enable to constrain the magnitude of collisional forces related to the African/Eurasian collision. Direction and magnitude of ridge push is relatively well constrained, as also is the direction of convergence between Africa and Eurasia. Since the orientation and local regime of the present-day stress field is well determined, the magnitude of the collisional forces remains the only unknown parameter: larger forces predict that larger parts of the peninsula are dominated by ~N140° Sh_{max}, whereas smaller forces predict a larger part with EW-oriented Sh_{max}. Although sensitivity of the stress field in mainland Iberia to different values of plate boundary forces along this segment is limited, the best fit between model results and observations on the orientation of Sh_{max} is obtained with collisional forces of ~$1.5x10^{12}$N/m near Tunisia gradually decreasing westward to 0.1 $x10^{12}$N/m near the Gloria Fault applied to the southern border of the model reflecting the rotational convergence of Africa with respect to Europe. This estimate of the collision forces along the southern boundary is of the same order of earlier estimates by Gölke & Coblentz [1996] and Jimenéz Munt [1999].

Incorporating stresses induced by lateral density variations

Topography has been sampled from the ETOPO5 database [Mueller *et al*., 1995], filtered with a 100km wavelength. Crustal thickness has been calculated using the Airy isostatic principle and a reference density of 2700kg/m^3.
The results (Figure 6.2.2b) predict that in large parts of Iberia extension is dominant. Although the orientation of the maximum horizontal compression is very similar to the results for the model without the induced stress fields (see Figure 6.2.2a), the stress field is much less homogeneous. This matches better the observed stress regimes (actual states of stress) in each region (larger arrows), ranging from uniaxial compression in the Betics and Alboran to predominantly strike-slip in the northwestern part of the peninsula and extension in central and northeastern Spain.
The orientation of the stress field and the actual state of stress predicted by the model resemble also closely the observations beyond the Iberian Peninsula. When the results for a larger part of the model are examined (Figure 6.2.3) and compared with the observations by De Vicente *et al.* [2000], a very acceptable fit is observed.

Conclusions:
Including forces related to lateral density variations does not change the trend of the maximum horizontal compression direction in the Iberian Peninsula significantly. This is due to the fact that the major lateral changes in the crustal thickness occur nearly perpendicular to the regional Sh_{max}. Therefore, the tensile stresses related to for example the northern and western margin of Iberia are sub-parallel to Sh_{max} and result in a reduction of the magnitude, but not in a significant rotation of Sh_{max}. Fit between the model results and the observed state of stress is generally improved by incorporating the induced stress.

6.3 Middle Miocene (Serravalian, ~12Ma) stress field

Observations, model geometry and boundary conditions

As the Middle Miocene is a period of major intraplate activity in the Iberian Peninsula (see Chapter 5), the stress field is relatively well documented. This enables validation of a few different scenarios with varying boundary conditions along the plate boundaries.

Boundary conditions:
The western boundary of the model is represented by the position of the Mid Ocean Ridge 12 Ma ago, defined by the 12Ma isochron of the oceanic crust [Mueller *et al.*, 1995]. Ridge push forces vary from 2.9x10^{12}N/m in the south and diminish gradually along the ridge towards the north to 1.1x10^{12}N/m near Iceland (see Appendix A for calculation). The northern border runs from the Mid Atlantic Ridge near Iceland north of Norway. The eastern border is defined along the Adriatic block, the curved front of the western Alps to the northern Alpine front. From there, an arbitrary boundary is chosen, more or less coinciding with the Carpathian front (see Bada [1999]). In the southeast of the model, active extension due to slab rollback of an active subduction process is documented and thus outward pointing forces have been applied to the Calabrian and Adriatic units in all of the scenarios.
The exact location of the southern border is more difficult to trace. In southern Iberia, a collision between the Betic/Alboran and Iberian mainland is observed but activity along this zone diminishes to the east near the Baleares. Contemporaneously, the African foreland is actively deforming as well. This front has been chosen to represent the southern border. A lively debate is still going on on the origin of the extension in the

Alboran block in this convergent setting (see e.g. Vissers *et al.* [1995]; Biermann [1995]; Lonergan & White [1997]; Balanyá *et al.* [1997]). To test several of the proposed settings for this southern segment, a range of scenarios has been applied. Some illustrative results will be presented to show that constraints on the tectonic evolution of the region can be inferred from confronting results of numerical modelling with the reconstructed stress field.

Model results

For the different scenarios, ridge push forces have been kept constant. 1.0×10^{12}N/m outward forces simulate extension along the eastern part of the model (Adria) and 1.0×10^{12}N/m forces applied to the boundary of the model simulate compression along the Alpine front.

Scenario1 (Figure 6.3.1a): Any influence due to the collision of the Betics and Iberia and the extension in the Alboran domain is neglected. Collisional forces related to collision with Africa and the Alps are the only far field forces applied to the boundaries of the model. The resulting stress field (Figure 6.3.2a) is very homogeneous throughout the entire model with a predominantly ~N160^o oriented σ_1. Along the Alpine front, the orientation of σ_1 turns perpendicular to the front. Active near E-W extension to the east of Sardinia and Corsica is coinciding with the observations. However, this scenario has to be disregarded due to the misfit in the Alboran domain.

Scenario2 (Figure 6.3.1b): Extension along the southern border (1.0×10^{12}N/m), compression along the Betic front (1.0×10^{12}N/m).

The results (see Figure 6.3.2b) show a stress field in Iberia with a WNW-ESE oriented σ_1 and N-S oriented extension in the entire Mediterranean basin. These results are in contrast with the observations, especially in Central Iberia and the southwestern part of the model.

Scenario3 (Figure 6.3.1c): Compression along the southern border of the model and the Betic front (both 1.0×10^{12}N/m). The directions of σ_3 in the Mediterranean Basin fit the observations, especially in the Tyrrhenian basin and eastern Alboran (see Figure 6.3.2c). The modelled stress field in the Alboran domain is however having a relatively large compression component with respect to the observations. The fit in mainland Iberia is good and comparable with the first scenario.

Scenario4 (Figure 6.3.1d): To simulate the active late stage extension in the Alboran basin in an active convergent setting, larger forces have been applied to the Betics and the eastern part (Kabylia) of the southern border (1.0×10^{12}N/m) than for the western part

Figure 6.3.1 (next page, see www.geo.vu.nl/~andb/iberia for full size, full color version)

Figure combining modelling results for different scenarios and observations of the stress field of the Middle Miocene situation (12 Ma). Thick arrows and lines show observed stress data and stress trajectories, small arrows show model predictions. See text for discussion. Insets show boundary conditions and distribution of young oceanic (intermediate gray), old oceanic (light gray), continental margin (white) and elevated continental (dark gray) regions. For all of the scenarios extension occurs along the Adria segment, and compression occurs along the Alpine front and ridge push occurs along the Mid Oceanic Ridge.

A) Scenario 1: compression along the Northern Africa segment.

B) Scenario 2: extension along the Northern African segment and northwestward compression along the Betic front.

C) Scenario 3: compression along the Northern African segment, otherwise as in scenario 2.

D) Scenario 4: smaller amount of compression (0.5×10^{12}N/m) along the western part of the Northern African segment, other boundaries as in scenario 3. Simulation of extension of the Alboran Basin in ongoing convergence between Africa and Eurasia.

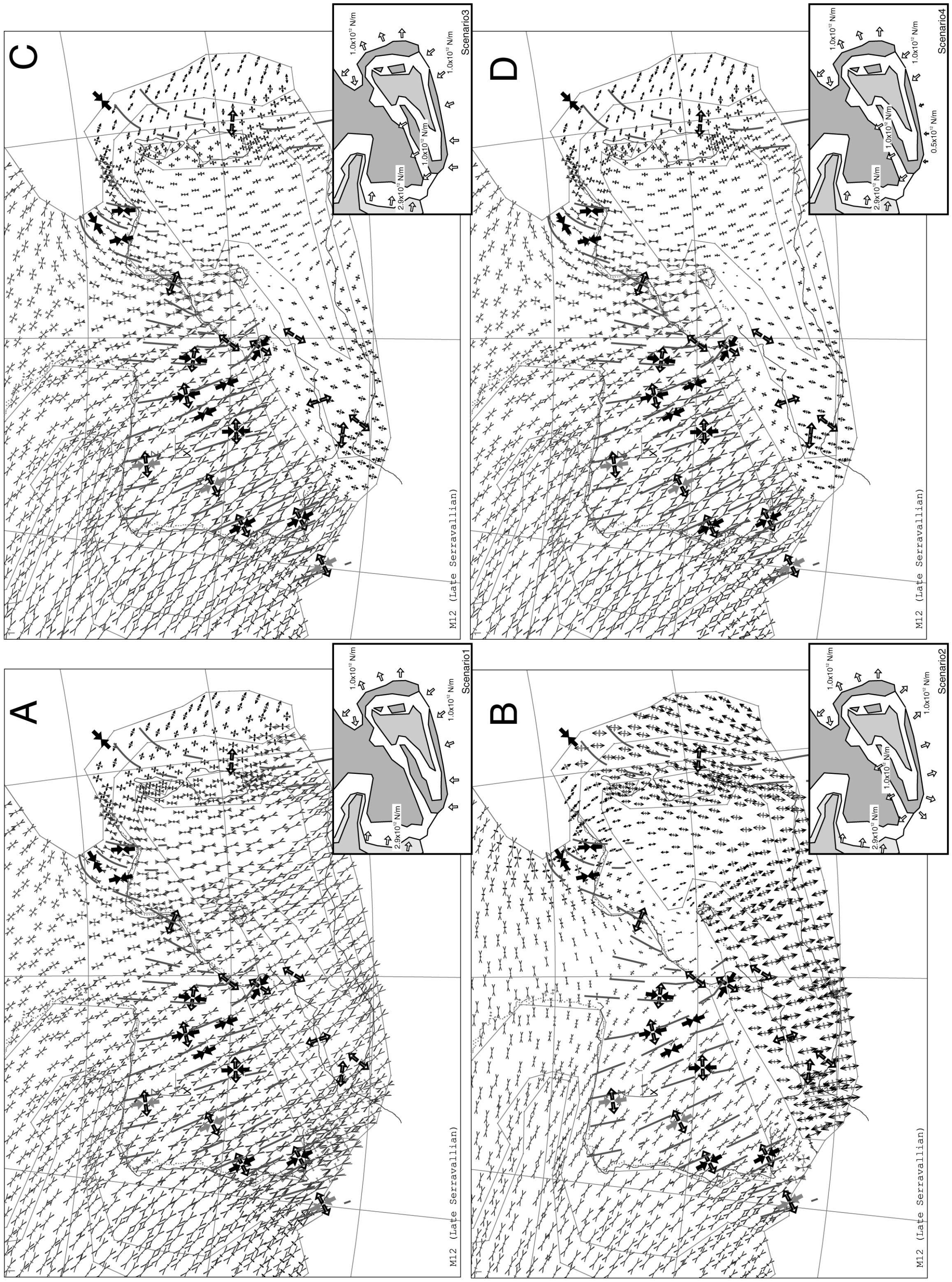
A
B
C
D
Scenario1
Scenario2
Scenario3
Scenario4
M12 (Late Serravallian)
M12 (Late Serravallian)
M12 (Late Serravallian)
M12 (Late Serravallian)

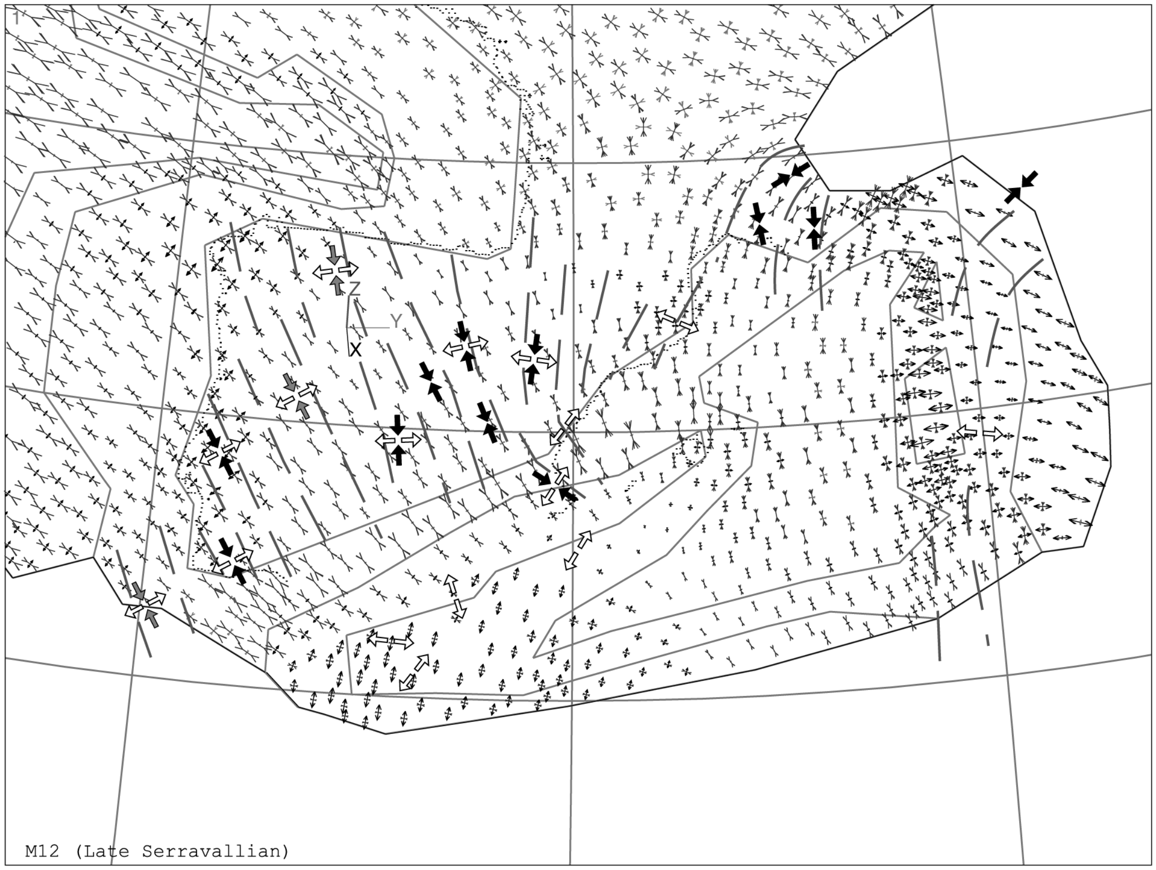

Figure 6.3.2 (see www.geo.vu.nl/~andb/iberia for full size, full color version).
Stress field for scenario4 when including potential energy calculations and paleotopography as shown in Figure 6.1.1b. See text for discussion.

of the southern border (Morocco, $0.5x10^{12}$N/m). The fit between results and observations is good for the entire model (see Figure 6.3.2d). Minor differences can be observed in the results with respect to scenario 3 (compare Figure 6.3.2c and 6.3.2.d). For the latter, in the Alboran basin extension is dominant, as is observed.
For scenario 4, the contributions of different types of possible activity (in sign – compression or extension- and magnitude) of the Calabrian segment or the Gloria fault on the intraplate stress field in Iberia has been tested. The influence of changes in these boundary conditions on the resulting stress field is very small and, therefore, the tectonic activity along these segments can be neglected in the calculation of the stress field in Iberia.

The fit of the modelled stress field is rather good, both in orientation of Sh_{max} as for the state of stress in different regions. An exception in all of the models is the anticlockwise rotation of predicted trajectories for Sh_{max} with respect to the observations in the northern segment of the Iberian Peninsula. Another misfit -as for the present-day situation- is that the observations show a rotation of the stress field perpendicular to the Pyrenees, which is not predicted by the model. This is due to the major weakness zone formed by the Pyrenean suture (see superficial seismic activity in Figure 2.4.1.4) that has not been included in the model, but tends to rotate the stress field perpendicular to it. The best fit in the southern part of the model is obtained in scenario 4 by simulating the extension in the Alboran block by applying larger collision forces along the western Betics front than along western Africa.

Conclusion:

(a) The contribution of different types of activity of Calabria or the Gloria fault on the intraplate stress field in Iberia is of very minor importance. Therefore, from the modelling no conclusions can be drawn about the tectonic setting along these plate boundaries during this period.

(b) Comparison of the reconstructed and predicted stress field favors a scenario (scenario4) in which Eastern Africa exerted more compression on Europe than Western Africa. This suggests that Eastern Africa was already coupled mechanically to Europe while western Africa had not yet collided with Iberia. This is supported by the fact that large NNE-SSW trending crustal shear zones [De Larouzière *et al.*, 1988]; [Andeweg & Cloetingh, 2001] in the Betic/Alboran region only started to develop from the L. Miocene. These crustal shear zones decoupled the Morocco/western Betics from the Africa/eastern Betics.

Incorporating stresses induced by lateral density variations

Based on the data gathered for the geological reconstruction of Iberia, first order estimates of the paleotopography are presented in Figure 6.1.1b. The main part of Iberia is elevated several hundreds of meters, as for example in the Spanish Central System (over 1000m), the Cantabrian and Pyrenean, Toledo Mountains, and Algarve. The accuracy of the original data set is not likely to be much better than approximately 500m. Subsequently this set is filtered with a wavelength of 100 km. Scenario4, for which the best fit was obtained in the first run, is used in the calculations; compare Figure 6.3.1d with 6.3.2 to see the differences.

Although the orientation of the main axes of stress does not change significantly, in general the fit improves with respect to the local state of stress. A few examples:

(a) Along the western margin of Iberia the results show an important extension component, as is observed.

(b) The E-W oriented extension in the Corsica/Sardinia/Tyrrhenian area increases with respect to the model without induced stresses.

(c) In the Alboran domain, extension in the basin is partly counteracted by induced compression, while in the thrust belts compression is reduced by induced near-parallel extension.

(c) In the northeastern Peninsula, nearly NS-compression is still dominant, but an important EW-extension is added when induced stresses are incorporated. This fits with observations in this area. Moreover, a slight clockwise rotation (up to 5 degrees) with respect to the model without induced stresses can be observed in this area. This rotation can be related to the elevated Pyrenees, which induces perpendicular extension.

As a general conclusion: as for the model for the present-day stress field, the fit to the observations is improving when stresses induced by lateral density variations are included in the model.

6.4 L. Oligocene (~24Ma) stress field

Observations, model geometry and boundary conditions

The western boundary, representing the Mid-Atlantic Ridge is located at the 24Ma isochron of the oceanic crust [Mueller *et al.*, 1995]. Ridge Push forces along this boundary vary from 2.7×10^{12}N/m near the Azores to 0.7×10^{12}N/m near Iceland (see Appendix A). The northern boundary of the model is located near Iceland and north

Norway. Iberia is amalgamated to the Eurasian plate and activity decreased along the Pyrenean plate boundary.
The southeastern boundary of the model runs along the active subduction front along Corsica/Sardinia, extensional forces are applied to this part of the boundary to simulate the active extension in the Provencal-Ligurian Basin. From here, the eastern border runs along the Alpine front and an arbitrary line towards the east. The exact location and the activity of the southern border are badly defined. Significant deformation occurred in this region after the Oligocene (extension in a convergent setting), obscuring the older geological past in the area. The southern border of the model, therefore, has been chosen to connect the Azores in a straight line with the westernmost part of the subduction front. In fact, the geometry in this area may have been more complex with, for example, the existence of transform faults [Andeweg & Cloetingh, 2001]. Model results
Based on the known boundary conditions, a set of scenarios has been tested:

Scenario1 (Figure 6.4.1a): Forces related to this subduction process can vary, depending on amongst others convergence rate, age of subducting oceanic crust (see discussion by Bada [1999]). In this scenario compression (0.5×10^{12}N/m) is exerted along the subduction front (eastern border) of the model. This is not a very likely situation to have occurred, but is included to show the differences in results and give the reader an idea of the dependence of the results on the boundary conditions. The resulting stress field is very homogenous compression all over the model from the eastern border to the Mid Oceanic Ridge, oriented ~290N. With respect to the observations, the fit is very poor to even contradictory.
Scenario2 (Figure 6.4.1b): In this scenario, extension (0.5×10^{12}N/m) is exerted along the subduction front. In terms of tectonic setting this is very likely due to the documented fast retreat of the subduction front and the onset of opening of the Western Mediterranean basin. A slightly better fit is obtained for the eastern peninsula, but for the rest the fit is not improving with respect to scenario1.
Scenario3 (Figure 6.4.1c): as scenario2, but compression (1.0×10^{12}N/m) exerted perpendicular to the southern boundary of the model. This compression can be explained in terms of early interaction between the African and Eurasian plates. Although still poor, the fit between model results and observations improves for large parts of the studied region. Especially, the fit in the southern, central and eastern peninsula is acceptable, just as in the opening Mediterranean basins. In the northern peninsula the fit remains poor.
Scenario4 (Figure 6.4.1d): as scenario3, but southward compression (0.5×10^{12}N/m) added in Pyrenees. Although the last major deformation in the Pyrenees has ended by Oligocene times, some reminiscent compression might be present (see Chapter 5). A small counterclockwise rotation (up to 15 degrees) of the orientation of maximum horizontal compression is improving the fit between observation and model result slightly.

Model results

No reasonable fit is obtained for any of the basic scenarios that have been applied (scenarios 1 and 2, Figure 6.4.1a and b). The misfit between model results and observations is enormous, up to perpendicularity between both. An additional force along the African plate boundary at the SW extreme of the Iberian Peninsula (as in scenarios 3 and 4, Figure 6.4.1c and d) does improve the fit significantly. The observed patterns of the stress field in the north are not matched by any of the scenarios.

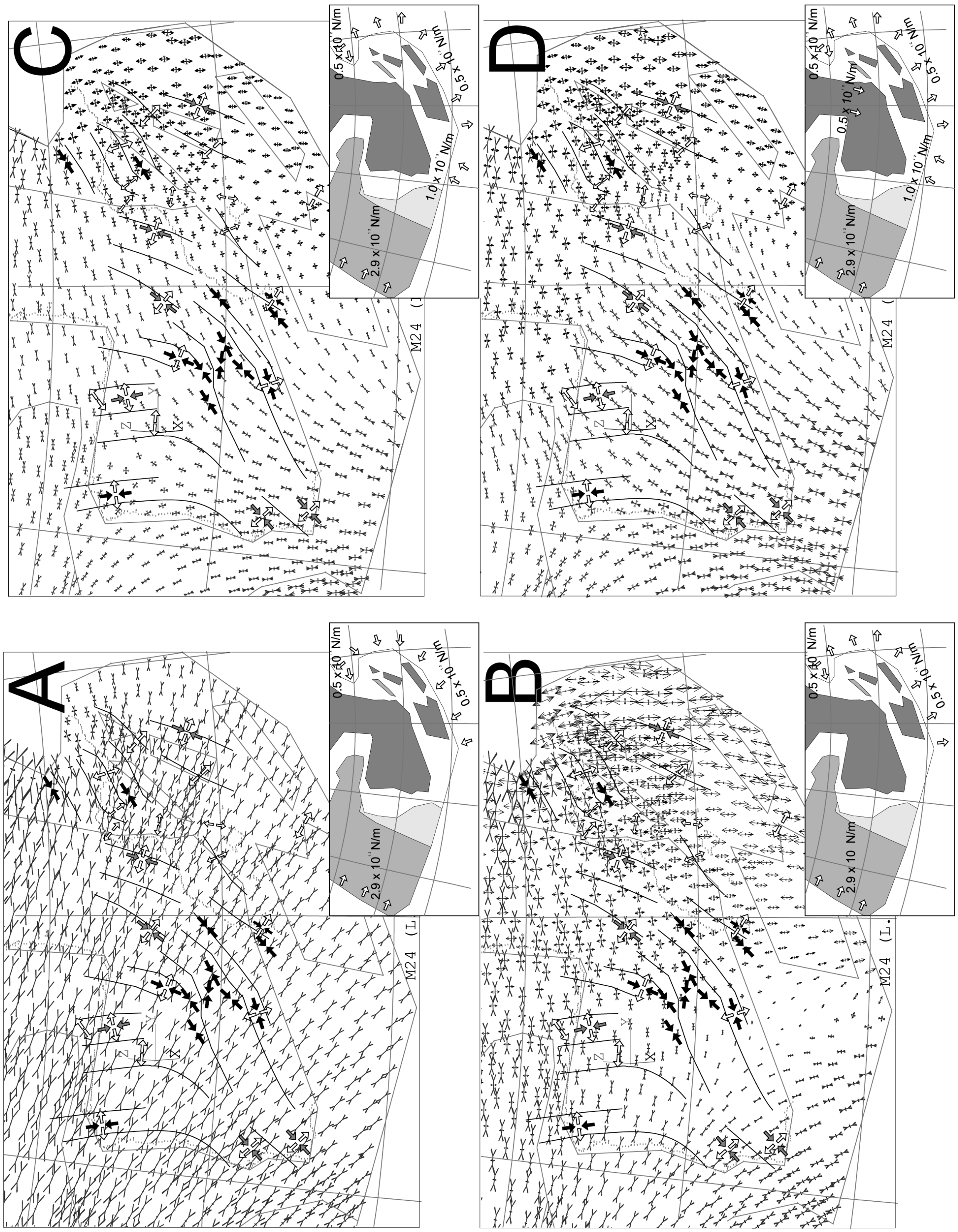

Figure 6.4.1 (see www.geo.vu.nl/~andb/iberia for full size, full color version).
Stress field results for different scenarios at 24Ma, see text for explanation. Insets shows boundary conditions for the different scenarios and distribution of young oceanic (intermediate gray), old oceanic (light gray), continental margin (white) and elevated continental (dark gray) regions. Thick arrows and lines show observed stress data and stress trajectories, small arrows show model results. Panels A and B: scenarios without compression along the southern border, compression along the eastern border for A, extension for B. Panels C and D: scenarios including compression along the southern border. In scenario of panel D compression in Pyrenees is included.

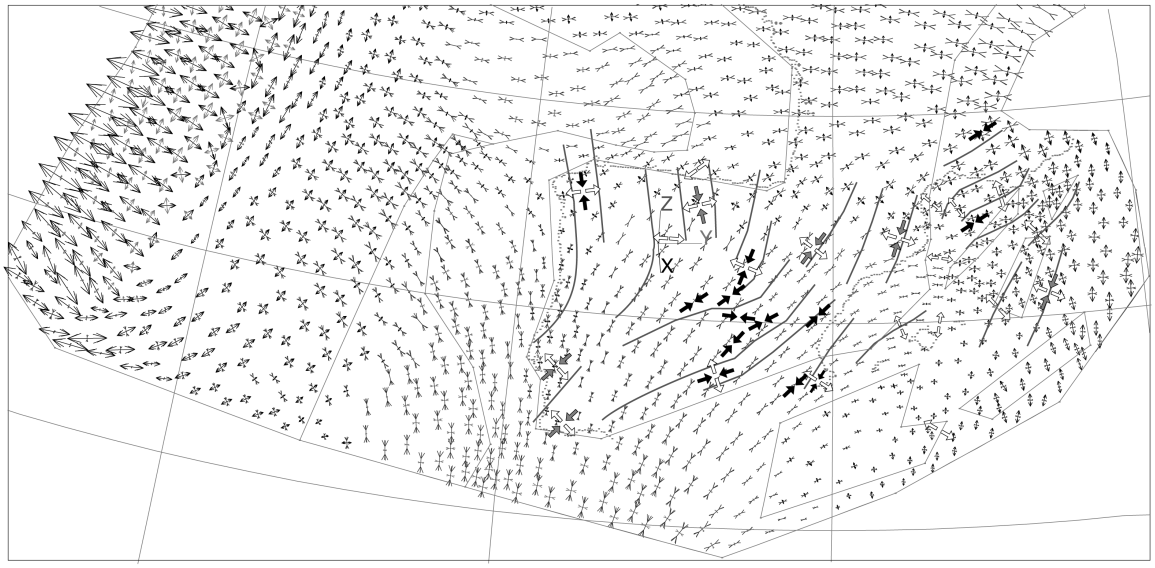

Figure 6.4.2 (see www.geo.vu.nl/~andb/iberia for full size, full color version).
Stress field for scenario when including potential energy calculations and paleotopography as shown in fig. 6.1.1c. See text for discussion.

Conclusion:

(1) The segment of the plate boundary SW of Iberia (Gorringe Bank) was an active zone of collision at the onset of activity of the plate boundary along the southern border of Iberia. Clockwise rotation of Iberia, partial decoupling along the western margin.

(2) Limited active convergence along the Pyrenean plate boundary did occur, including the Cantabrian Cordillera.

Incorporating stresses induced by lateral density variations

Based on the data gathered for the geological reconstruction of Iberia, first order estimates of the paleotopography are presented in Figure 6.1.1c. The Pyrenees, Cantabrian Cordillera and Iberian Chain are elevated regions. Because the results from the first series of models were non-exclusive about the boundary conditions and results, the conclusions that can be drawn from the results when incorporating the induced stresses cannot be but limited.

In general, the fit is slightly improved. For some regions the results are close to the observations, as for example in the northern and eastern part of the Peninsula and the Gulf of Lions. Due to the topography in the Pyrenees and Cantabrian Cordillera, a rotation of Sh_{max} towards a more N-S trend (parallel to the topographic gradient) can be observed.

Additional forces (compression along the southern segment) have been applied that were not expected based on paleo-geographical reconstructions, but still the stress field in this period can only partly be predicted by the finite element modelling. Either the data on the stress field is not accurate for this period (difficulty with dating of sediments and, therefore, stress fields as discussed earlier), additional processes that can act as stress sources have been active during this period, or the geometry of the southern border of the model is not well represented.

6.5 L. Eocene (~36Ma) stress field

Observations, model geometry and boundary conditions

The extent and quality of the reconstructed stress field is limited. The northern border of the model is the active convergent plate boundary running from the Pyrenees passing through the actively spreading King's Trough to the Mid-Atlantic Ridge. The western boundary is defined by the 36Ma isochron of the oceanic crust [Mueller *et al.*, 1995]. Ridge push forces have been determined using the formulas in Appendix A and equal 2.45 x 10^{12}N/m, directed perpendicular to the boundary. The southern boundary is an active subduction front southeast of Corsica/Sardinia and the Betic/Alboran block. As discussed before: forces related to subduction can vary. To test the effect of these several possibilities on the stress field, three settings have been tested for this boundary. Additionally, collisional forces related to the Pyrenean collision have been varied. This leads to the following set of scenarios:

<u>Scenario 1 (Figure 6.5.1a)</u>

Compression (1.0 x 10^{12}N/m, directed N320^{o}) along the southeastern border. The compression related to the Pyrenean compression is directed 180N, and has in scenario 1a a value of 2.0 x 10^{12}N/m, and in scenario 1b doubled to 4.0 x 10^{12}N/m.

<u>Scenario 2 (Figure 6.5.1b and c)</u>

No forces along the southeastern border. Compression related to the Pyrenean collision is directed 180N, and has in scenario 2a a value of 2.0 x 10^{12}N/m, in scenario 2b is doubled to 4.0 x 10^{12}N/m.

<u>Scenario 3 (Figure 6.5.1d and e)</u>

Extension (0.5 x 10^{12}N/m, directed N140^{o}) along the southeastern border. Compression related to the Pyrenean collision is directed N180^{o}, and has in scenario 3a a value of 4.0 x 10^{12}N/m, and in scenario 3b is half of that (2.0 x 10^{12}N/m).

Model results

In general, a rather good fit is obtained for the eastern part of the model for any of the applied scenarios. For scenarios 1b and 2a compression is equally present throughout the entire Peninsula. This seems to be in contrast with the observations: more intense deformation is observed along the northern rim, diminishing southward. If levels of compression in the southern peninsula had been at equal levels as in the north, major compressional deformation would be expected in this region as well. Therefore, based on the observations, scenarios 1b and 2a are less likely. Based on the magnitudes of stresses in the Betic/Alboran block, scenarios 2b, 3a and 3b are favored. Inclusion of extensional forces along the southeastern rim (scenario 3) improves the fit of the predicted stress field with the observed stress field slightly in the central and northeastern part of the model, but causes an increasing misfit in the northwestern peninsula by a clockwise rotation of the orientation of maximum horizontal compression. For scenario 3a, the fit in northwest Iberia is poor in comparison with scenarios 2b and 3b. Distinguishing between the latter two is not possible on basis of the model results. Therefore, a best fit can be obtained by application of collisional forces of the Pyrenees having a value of 2.0 x 10^{12}N/m in combination with no or limited extensional forces at the southeastern boundary.

Conclusions:

(a) Plate boundary activity along the southern boundary was limited.

(b) Collisional forces related to the Pyrenean collision are of twice the order of the present collisional forces associated with the African/Eurasian convergence.

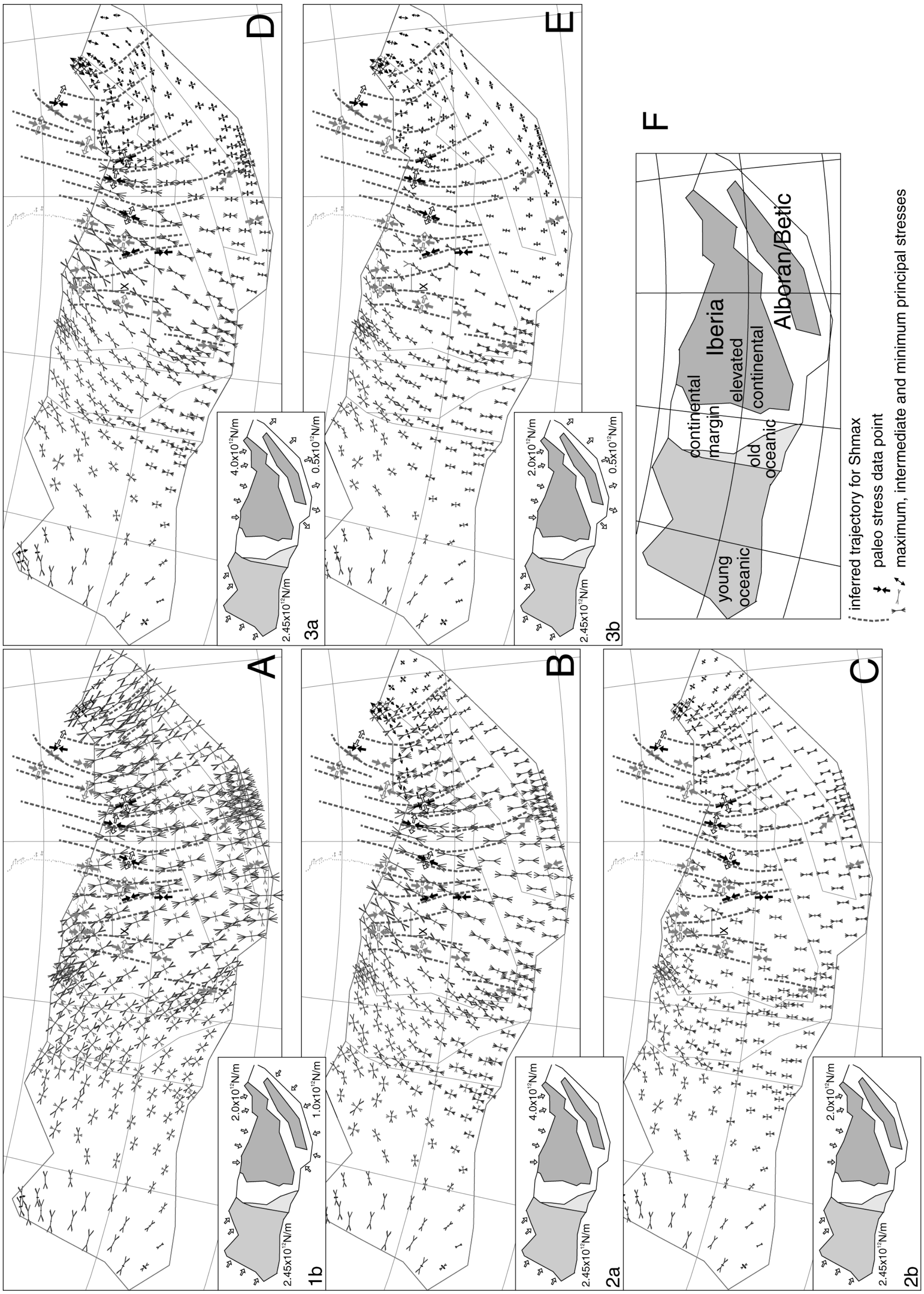

Figure 6.5.1
Stress field results for different scenarios at 36Ma. Insets shows boundary conditions for the different scenarios and distribution of young oceanic (intermediate gray), old oceanic (light gray), continental margin (white) and elevated continental (dark gray) regions. Thick arrows and lines show observed stress data and stress trajectories, small arrows show model results. See text for discussion of scenarios.

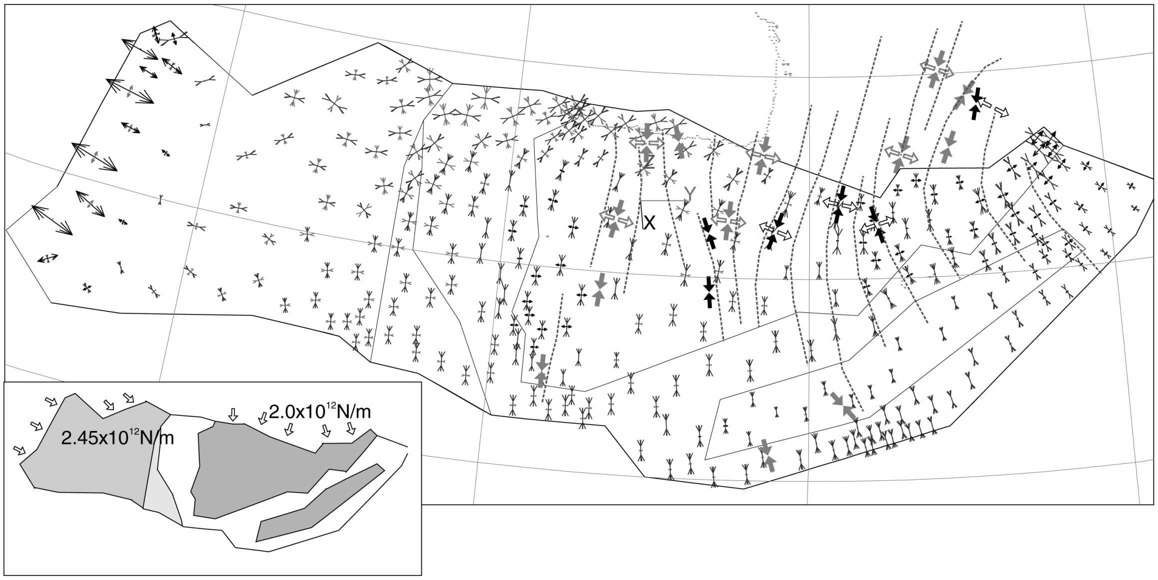

Figure 6.5.2
Stress field for scenario4 when including potential energy calculations and paleotopography as shown in fig. 6.1.1d. Compare to results of Figure 6.5.1. See text for discussion and www.geo.vu.nl/~andb/iberia for full size, full color version.

Incorporating stresses induced by lateral density variations

First order estimates of the paleotopography are presented in Figure 6.1.1d. Major topography was present in the Pyrenean and Alboran regions, and the Cantabrian Cordillera and Iberian Chain started to become elevated areas. Main part of Iberia was just a few hundreds of meters above sea level. When this database is used for the calculation of the induced stresses, main differences with the models without induced stresses are observed at:

(a) the Mid Atlantic Ridge (extension),
(b) the western margin of Iberia. Because the margin is parallel to the regional stress field predicted by the model without induced stresses, Sh_{max} is hardly affected. Sh_{min} is however reduced from compression to extension perpendicular to the margin.
(c) the Alboran block, compression is reduced nearly 50%.
(d) the Pyrenees. The state of stress changes to strike-slip, as is observed.

Apart from the Pyrenean region, it is not possible to determine whether the results are improving including the induced stresses.

The stresses induced by the elevated topography (and therefore pronounced crustal thickness) in the Alboran units seem not to be large enough to start extensional collapse of the thickened orogen in this region as suggested by Vissers *et al.* [1995]. A trigger in the form of the southwestward migrating extension from the Rhone graben and Valencia Trough might have contributed to the onset of large-scale extension in this area. However, more detailed analysis of this problem is required to discriminate between these models.

6.6 L. Paleocene - E. Eocene (~54Ma) stress field

Observations, model geometry and boundary conditions

The western boundary is defined by the 54Ma isochron of the oceanic crust [Mueller *et al.*, 1995]. Ridge push forces have been determined using the formulas in Appendix A and equal 2.1 x 10^{12}N/m, directed perpendicular to the boundary. Collision along the northern plate boundary just started. Collision along the eastern part of the southern boundary is inferred from crustal thickening in the internal zone of the Betics. The eastern border is starting to develop as a left-lateral transform fault between the Pyrenees and the Alpine ranges. Along the southeastern boundary subduction is active. Forces related to subduction can vary from extension (trench suction) to compression (subduction resistance).

Model results

Four scenarios have been tested for different settings of activity along the southern borders of the models. For all of the scenarios, a value of 2.1 x 10^{12}N/m for ridge push is included, as is 1.0 x 10^{12}N/m along the northern segment to simulate the onset of collision between Eurasia and Iberia.
Scenario1 (Figure 6.6.1a): As a reference model, no additional forces have been applied.
Scenario2 (Figure 6.6.1b): 0.5 x 10^{12}N/m outward pointing forces have been applied to the southeastern border to simulate trench suction in this area.
Scenario3 (Figure 6.6.1c): 0.5 x 10^{12}N/m inward pointing forces have been applied to the southeastern border to simulate subduction resistance in this area.
Scenario4 (Figure 6.6.1d): 0.5 x 10^{12}N/m inward pointing forces have been applied to the southern border to simulate coupling with the African plate in this area.

When compared with the observed stress field, scenario 2 yields solutions nearly perpendicular to the observations and therefore should be disregarded. For any of the other scenarios, the orientation of the modelled stress field is comparable with the observations in the eastern most part of Iberia. Large differences in the modelled results can be seen in western Iberia. The fit to the observations is poor for scenarios 1 and 3 and reasonable for scenario4 .
Therefore, based on the amount of deformation in this period and the direction of the principal axes of stress, scenario4 is favored. A better fit can be obtained by including a push along the Gorringe Bank area, which is supported by geological indications for inversion in this area (see Chapter 4). This implies that plate interaction between the Iberian and African plate must have been active this period.

Figure 6.6.1 (next page, see www.geo.vu.nl/~andb/iberia for full size, full color version)
Stress field results for different scenarios at 54Ma. Insets show boundary conditions for the different scenarios and distribution of young oceanic (light grew), continental margin (white) and elevated continental (dark grew) regions. Thick arrows and lines show observed stress data and stress trajectories, small arrows show model results.
A) Scenario 1: compression along the northern and western border (simulating start collision with Eurasia and ridge push, respectively).
B) Scenario 2: similar to scenario1, added light tension along the eastern border (simulating trench suction).
C) Scenario 3: similar to scenario1, added small amount of compression along eastern border (simulating subduction resistance).
D) Scenario 4: similar to scenario1, added compression along the central southern section (simulating collision with the African plate).

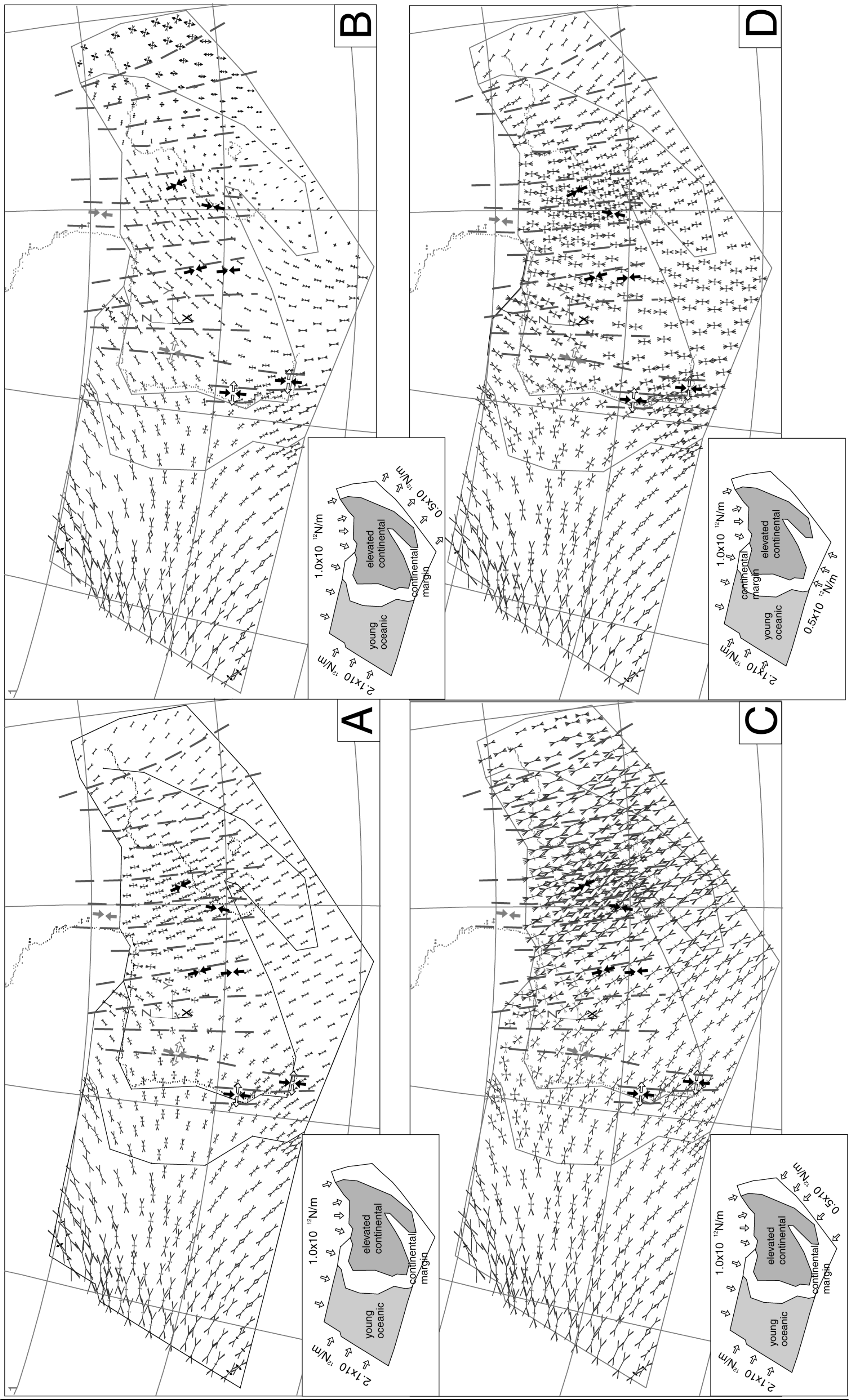
B
D
A
C
1.0x10 12N/m
0.5x10 12N/m
2.1x10 13N/m
elevated continental
continental margin
young oceanic

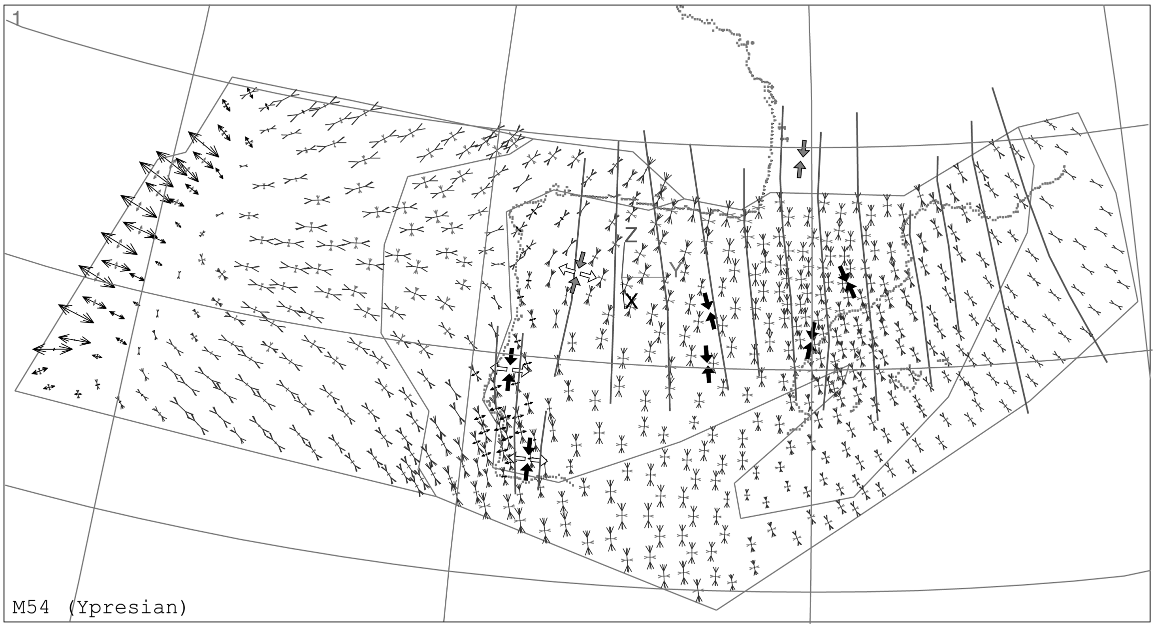

Figure 6.6.2 (see www.geo.vu.nl/~andb/iberia for full size, full color version)
Stress field for scenario4 when including potential energy calculations and paleotopography as shown in Figure 6.1.1e. When compared with Figure 6.6.1d, small differences can be observed for the western margin of Iberia and the southern segment of the model. See text for further explanation.

Incorporating stresses induced by lateral density variations

Based on the data gathered for the geological reconstruction of Iberia, first order estimates of the paleotopography are presented in Figure 6.1.1e. Mainland Iberia was only slightly elevated above see-level, no major mountain belts were present. The major trends in crustal topography are perpendicular to the general trends in the stress field obtained by the first run of modelling. This leads in general to lower levels of intraplate stress for the continental parts and higher levels in offshore parts, see for example the western Alboran block in Figure 6.6.2 (in comparison with Figure 6.6.1d). The orientation of Sh_{max} is hardly affected by the stresses, but the state of stress changes in for example the western Iberian margin from nearly uniaxial compression to a strike-slip regime. The quality of the reconstructed stress field and the reconstructed crustal setting are too poor to draw more detailed conclusions from the model results.

6.7 General results and conclusions

As shown by the modelling results, modelling of the (paleo)stress field as presented in this Chapter enables quantative evaluation of the many qualitative paleogeographical models. Validity of these models can be tested by confronting the results of suggested different geometries and plate boundary activity on the stress field with the observations. Although conclusions about the tectonic setting cannot be more detailed than the input data, some of the proposed paleogeographical models can, based on the modelled stress field, be classified as ‘unlikely’. Conversly, the modelling can be used to obtain additional constraints on the tectonic evolution of the western Mediterranean. For the 24Ma and 54Ma models, non-documented plate interaction is inferred from the additional compression in the southern parts of the models that is required to obtain a reasonable coherence between model results and observations. Thus interaction along the border between the African and Iberian/Eurasian plate likely occurred throughout the entire Cenozoic.

Although the model is very straightforward basic and disregards some of the processes that contribute to the stress field (see section 2.3), it is very well able to predict the general trends in the observed stress field. Local observations of stress in the field will most likely differ from the general trend predicted by the model, due to the existence of crustal inhomogeneities or faults that are not incorporated in the model. It is possible to obtain better fits between results and data by adding extra (undocumented) variations in the stress sources and geometries, but this is not presented here because the quality and quantity of input data is limited. More observations of the stress field through geological history are required to draw more detailed conclusions from the modelling about the forces and activity at plate boundaries. More importantly however, the model shows how the stresses would be oriented if the Earth's lithosphere acted as an elastic plate of 100km thickness. Since this is only an approximation of the behavior of the lithosphere, it would not be of added value to fine-tune the results until a perfect fit is obtained.

Including stresses induced by lateral density variations in general provides less homogeneous stress fields, which fit the observed stress fields much better. For the entire model for the present-day stress field, the model predictions match the observations reasonably. This fit implies that the concept can be applied for the geological past.
In many cases, the gradients in topography are found to be parallel to the general stress field obtained by the modelling without including the induced stresses. Therefore, including the induced stresses often does not affect the orientations of the principal axes of stress, but results in other ratios between these (changing from uniaxial compression to pure strike-slip, for example). When the induced stresses are large and opposite to a weak 'far-field' stress, they can provoke an interchange between the σ_1 and σ_3 axes.
The results can be interpreted in a general way to gain insight in first order (paleo)topographic patterns. An improved fit to the observations by a reorientation or change of the predicted stress field can be observed when large crustal edifices as for example the reconstructed Pyrenees at 24Ma are included. The conclusion from these results cannot be more detailed than that the Pyrenees formed an elevated ridge during this period, but in this way independent estimates on paleotopography can be provided.

The 2D models presented are able to predict the observations reasonably. Before a step to fully 3D models makes sense, more precise data on density variations (lateral and vertical) and independent data on lithosphere and crustal thickness are required [Andeweg *et al.*, 1999b]. As these data will be available only for the present-day situation, one might wonder whether a complex 3D model would help in understanding the evolution of the stress field through the geological past in Iberia.